Bats-inspired Frequency Hopping for Mitigation of Interference between Automotive Radars

Jonathan Bechter, Carmen Sippel, and Christian Waldschmidt
Institute of Microwave Engineering, Ulm University, Germany
Email: jonathan.bechter@uni-ulm.de

***Abstract*—It was reported for specific bats, that they use a certain scheme to shift the frequencies of their echo location calls to counteract interferences with conspecifics. As in road traffic, an increasing number of cars is equipped with radar sensors, there is also the problem of mutual interference. The available frequency bands are limited, so a randomized frequency hopping will not be the best solution. In this paper, we adapt the frequency hopping behavior of the bats reported in [1] to a radar system. We discuss the algorithm and show measurements of its performance in an anechoic chamber.**

I. Introduction

A. Interference between Automotive Radar Sensors

A typical modulation scheme in automotive radar is the FMCW or chirp sequence modulation, in which the sensors transmit linear frequency ramps. When multiple of such radar sensors operate in the same frequency band, interference occurs. This interference is commonly limited in time with a high amplitude, and it will lead to an increased noise floor in the spectrum [2]. A possible interference scenario is shown in Fig. 1. The black and the red frequency ramps belong to two different sensors. When the frequencies are similar to a certain point in time, interference occurs.

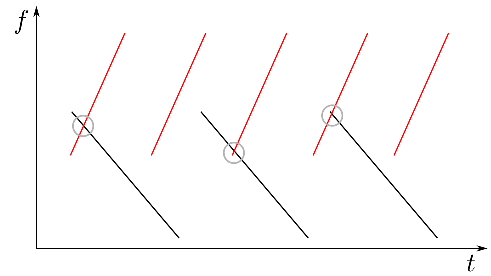

Fig. 1. The frequency ramps of two chirp sequence modulated radar sensors (red and black) overlap in time and frequency, leading to unwanted interference in multiple ramps (gray circles).

B. Jamming Avoidance between Bats

A group of researchers investigated jamming avoidance responses (JAR) of bats. The bats transmit frequency chirps for their echolocation calls. When interference with conspecifics occurs, the European bat *Tadarida teniotis* uses frequency hopping to avoid this interference. The bats do not shift their call frequencies in a random way. Instead, the bat with the higher frequency will shift its frequency upwards, while the bat with the lower call frequency shifts it downwards, see [1].

This behavior will lead to interference free operation with a higher rate of success than switching transmit frequencies at random, especially when the available bandwidth is limited. As the frequency bands for automotive radar are narrow compared to typical radar bandwidths, e.g. 200 MHz in the 76-77 GHz band, we adapted the bats' behavior for radar applications.

II. Adaptation of the Bats' Frequency Hopping

In the following section, it is described how the frequency behavior of the bats can be adapted to an automotive chirp sequence radar. The steps required are a detection of interference in the baseband signals of all frequency ramps, followed by a correlation of the interfered time domain samples with their corresponding frequencies in the RF domain. With knowledge of the frequencies occupied by another sensor, a new center frequency for the next measurement is determined.

A. Determination of Interfered Frequencies

There is a direct coupling between the baseband time scale and the RF transmit frequency, given by the slope of the transmitted ramps. In Fig. 2, interference occurs between the frequency ramps Tx_1 and Tx_2 of two sensors. For the RF signal Tx_1 (upper graph), the baseband signal is also shown (lower graph). The sensor's receiver bandwidth limits the interference duration, shown in the green box. The interfered samples in the baseband signal correspond to a certain frequency range in the RF signal. An interference detection is performed for the baseband signal of each frequency ramp, e.g. with a power detector [3], and from the interfered time samples, the corresponding frequencies are calculated.

B. Changing the Transmit Frequency

If most interfered frequencies are detected below the own center frequency, the radar bandwidth is set above the highest frequency of detection. Otherwise, it is set below the lowest detection. To decide which option is correct, we calculate a center of interference similarly to the center of mass of a homogeneous object as

$$\hat{r} = \frac{1}{N_{\text{int}}} \sum_{i=1}^{N_{\text{int}}} \frac{s_i}{N}. \quad (1)$$

There, N is the total number of samples in a frequency ramp, N_{int} is the amount of interfered samples over all frequency ramps, and the s_i are the numbers of the interfered samples. Note that $\hat{r}$ is only an estimator for an optimum value r.

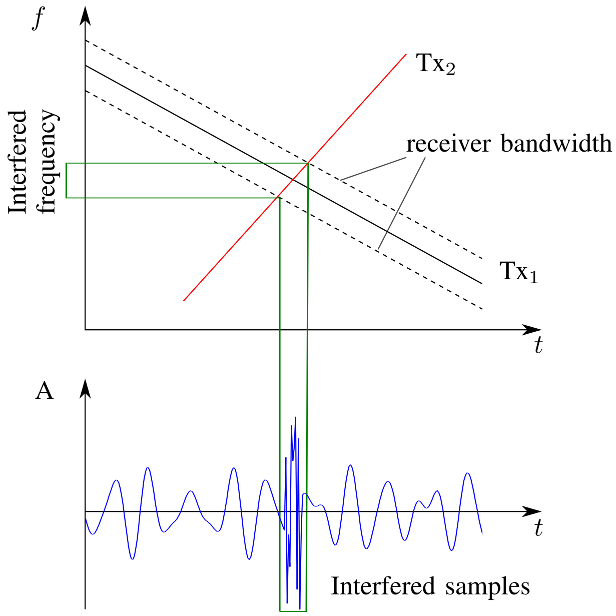

Fig. 2. The dashed lines in the top drawing show the receiver bandwidth of system Tx_1, which lead to the time limitation of the interference caused by the system Tx_2. The interference detected in the baseband signal (bottom) is directly correlated to a certain frequency range in the RF domain (top).

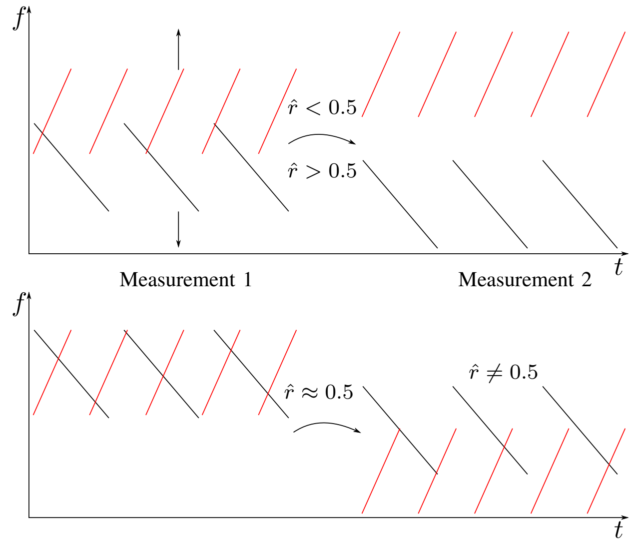

Fig. 3. Two examples show interference between the frequency ramps of two different sensors (red and black). Both use the bats' frequency hopping. In the upper drawing, there is a partial overlap in the bandwidth. This problem is solved with frequency hopping in the next measurement. In the lower drawing, both signals occupy exactly the same bandwidth. After a random frequency shift, the second measurement is similar to the initial scenario in the upper drawing.

A value of $\hat{r} < 0.5$ leads to an upward frequency shift, a value of $\hat{r} > 0.5$ leads to a downward frequency shift. The upper drawing of Fig. 3 shows a scenario, in which one sensor calculates $\hat{r}$ above, one below 0.5. In the following measurement, the sensors shift their transmit frequencies in the opposite directions and the interference is mitigated. If the sensors operate at similar center frequencies, we will have $\hat{r} \approx 0.5$, and no clear decision can be made. Therefore, if

$$|\hat{r} - 0.5| < \epsilon, \tag{2}$$

with an arbitrary ϵ, a random frequency shift will be performed. After one or both sensors did a random frequency shift, $\hat{r}$ is calculated again. The example in the lower drawing of Fig. 3 shows, how a random frequency shift can lead to the scenario in the upper drawing, which can be solved reliably.

III. Comparison with other Methods

We compare the method with other possible algorithms for frequency hopping. We set up a stochastic model which indicates the expected interference power during a measurement.

A. Model Description

We consider two sensors using the described method and a bandwidth of $B = 200\,\mathrm{MHz}$ in the 76-77 GHz band. When they operate at the same time, there is a certain probability that both bandwidths will overlap, if both sensors have random initial frequencies. We located one sensor arbitrarily at 76.5 GHz. The center frequency of the other sensor can take values from 77.1 to 77.9 GHz. Thus, the probability for occurrence of interference is

$$p_{\mathrm{Int}} = \frac{2B}{78\,\mathrm{GHz} - 77\,\mathrm{GHz} - B}. \tag{3}$$

It is important, which samples in the time domain signal are interfered, because the window function takes significant influence on the received interference power, compare [4]. We consider the von-Hann window frequency domain:

$$w(f) = \frac{1}{2} \cdot \left(1 - \cos\left(\frac{2\pi f}{B}\right)\right), \quad f \in (0, B). \tag{4}$$

For a certain frequency overlap f of the sensors' bandwidths, the expected interference power $\mathrm{E}(P_{\mathrm{int},f})$ is proportional to

$$\mathrm{E}(P_{\mathrm{int},f}) \propto \int_0^f w^2(\hat{f})\; d\hat{f}. \tag{5}$$

With the probability $p(f)$ of frequency overlap f, the expected overall interference power is

$$\mathrm{E}(P_{\mathrm{int}}) \propto \int_0^B p(f) \cdot \int_0^f w^2(\hat{f})\; d\hat{f}\; df. \tag{6}$$

If interference occurs, each overlap f has the same probability, so the overall probability for overlap f is

$$p(f) = p_{\mathrm{Int}} \cdot \frac{1}{B}. \tag{7}$$

For two sensors with $B = 200\,\mathrm{MHz}$, this leads to

$$\mathrm{E}(P_{\mathrm{int}}) \propto \frac{3B^2}{8 \cdot (78\,\mathrm{GHz} - 77\,\mathrm{GHz} - B)}. \tag{8}$$

This value describes the expected interference power between two sensors which transmit at random positions in the frequency band. With a probability p_{solve}, the frequency hopping solves the interference problem. But, it is also possible to

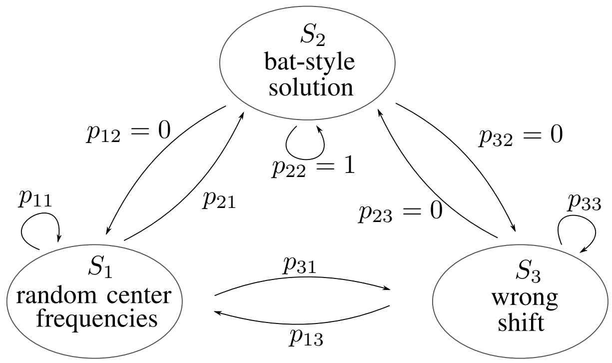

Fig. 4. State model to quantify the performance of the frequency hopping method.

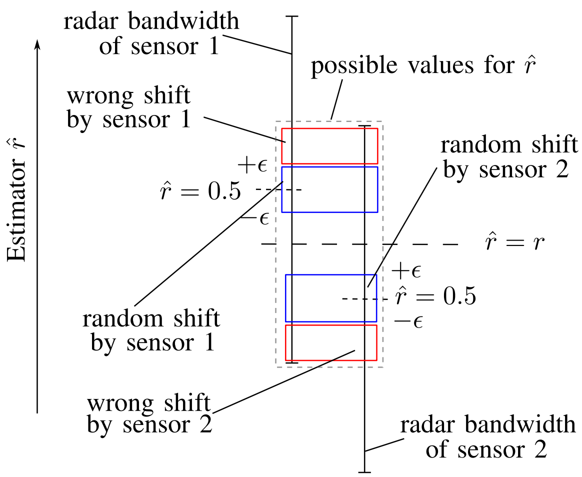

Fig. 5. $\hat{r}$ is limited to values within the gray rectangle for the given bandwidth overlap. If $\hat{r}$ is within the blue rectangles, a random frequency shift is performed. If it is within the red rectangle, a wrong decision is made, which means the frequencies of both sensors are shifted in the same way.

perform a random frequency shift according to (2) or to shift the frequency in the wrong direction, if the estimator $\hat{r}$ is bad. We consider these possibilities as states in the state model in Fig. 4. In the initial state S_1, the center frequencies of both sensors are random. After each measurement, this state can be reached with the condition in (2). If $\hat{r}$ allows application of the bats-adapted algorithm, state S_2 can be reached and no more interference is expected. If a frequency shift in the wrong direction is performed because of a bad estimation $\hat{r}$, the sensors shift their frequencies in the same direction. As the frequencies of interference detection are identical for both sensors, they set the center frequency to the same value in the next measurement. This leads to state S_3, in which both sensors have the same center frequencies and will detect the same interferences. Thus, from this state it is not possible to accomplish interference-free operation with the bat algorithm.

Fig. 5 shows, which values of $\hat{r}$ will lead to a random frequency shift or to a shift in the wrong direction. We model the probabilities for those $\hat{r}$ depending on the difference in center frequencies f_c of the sensors with two approaches. In the first approach, we assume that the repetition intervals of the frequency ramps of both sensors are identical, or multiples of each other. In this case, the same time samples will be interfered in each ramp, and the probability density of $\hat{r}$ corresponds to a uniform distribution. The expected value of $\hat{r}$ is r, and its variance is

$$\sigma^2_{\text{uniform}} = \frac{1}{12}(f_{c,1} + B/2 - (f_{c,2} - B/2))^2. \tag{9}$$

In the second approach, we assume that the repetition intervals of the frequency ramps are different and not multiples of each other. Then, the interfered samples in all ramps are uniformly distributed over the bandwidth common to both sensors. For a large number N of frequency ramps, e.g. 128, $\hat{r}$ is normally distributed according to the central limit theorem with variance

$$\sigma^2_{\text{normal}} = \frac{1}{N}\sigma^2_{\text{uniform}}. \tag{10}$$

With variance and expected value, we calculate the probabilities in Fig. 4 for a fixed ϵ. The probability of a certain state in the $i-$th measurement is described with a Markov chain as

$$P_i([S_1\ S_2\ S_3]) = [1\ 0\ 0] \cdot \begin{pmatrix} p_{11} & p_{21} & p_{31} \\ p_{12} & p_{22} & p_{32} \\ p_{13} & p_{23} & p_{33} \end{pmatrix}^i. \tag{11}$$

The expected interference power E_2 in state S_2 is zero, E_1 in state S_1 is given in (8). For state S_3, it is calculated as a special case of (5) with $f = B$, leading to

$$\mathrm{E}_3 \propto \frac{3}{8}B. \tag{12}$$

The expected interference power in measurement i is

$$\mathrm{E}_{\mathrm{Bat},i} \propto P_i([S_1\ S_2\ S_3]) \cdot [\mathrm{E}_1\ \ \mathrm{E}_2\ \ \mathrm{E}_3]^T. \tag{13}$$

We quantify the expected interference power for other frequency hopping algorithms in the same way. For an algorithm which performs a random frequency shift after each measurement, as described in [5], we set $p_{11} = 1$. An algorithm which performs a random frequency shift only if interference is detected, is described by changing p_{Int} to p^i_{Int} in (7), giving

$$\mathrm{E}_{\mathrm{Rand},i} \propto \frac{3B}{16} \cdot \left(\frac{2B}{78\,\mathrm{GHz} - 77\,\mathrm{GHz} - B}\right)^i. \tag{14}$$

Another method we want to compare is a standard which separates the frequency band into five equal slots, as mentioned in [6]. Each sensor uses a random slot, and changes to another random slot if interference occurs. In case of interference, the sensors' bandwidths overlap completely and the interference power is the same as in (12). The probability of occurrence of interference is 0.2, so the expected interference power is

$$\mathrm{E}_{\mathrm{Stand},i} \propto 0.2^i \cdot \frac{3}{8}B. \tag{15}$$

The expected interference power for a series of measurements is plotted in Fig. 6 with the variance of (10). In the initial measurement, two sensors use random center frequencies and bandwidths of 200 MHz in the $76 - 77$ GHz band. Integration of the curves gives a measure of the total expected interference power for each method, see Table I. For the bat method, results for both considered variances are given with their optimum values for ϵ.

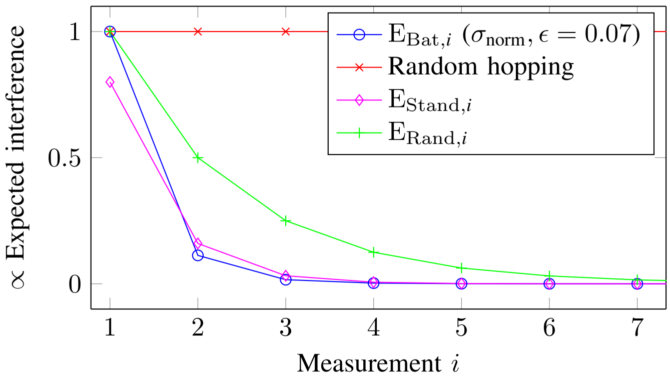

Fig. 6. Normalized comparison of the expected interference power in a series of measurements with different frequency hopping methods.

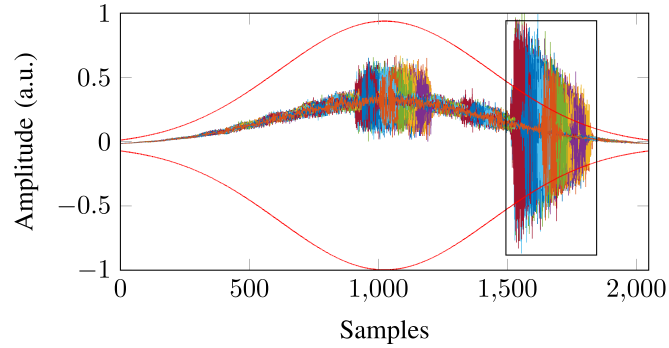

Fig. 7. Baseband signals of 128 frequency ramps of the interfered radar. The interferer operates from 76.4 to 76.45 GHz, the victim from 76.1 to 76.5 GHz. The detected interference is indicated by the black box.

TABLE I

TOTAL EXPECTED INTERFERENCE POWERS, NORMALIZED

$\mathrm{E}_{\mathrm{Stand}}$	$\mathrm{E}_{\mathrm{Bat}}, \sigma_{\mathrm{norm}}, \epsilon = 0.07$	$\mathrm{E}_{\mathrm{Bat}}, \sigma_{\mathrm{unif}}, \epsilon = 0.34$	$\mathrm{E}_{\mathrm{Rand}}$
1	1.13	1.77	2

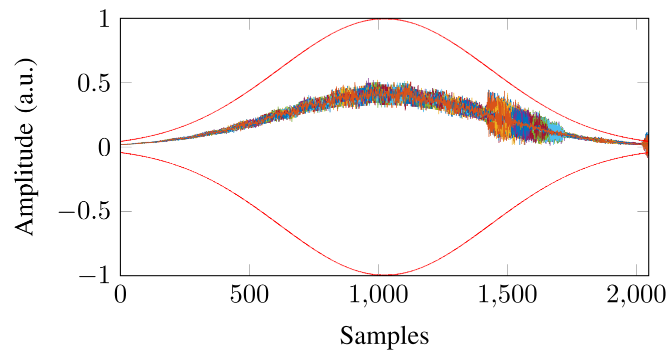

Fig. 8. According to the interference detected in Fig. 7, the victim changes its operation frequency to 76-76.4 GHz in the next measurement. The high amplitude interference is not present anymore.

IV. Experimental Validation

We show a measurement of a typical interference scenario, carried out in an anechoic chamber. The described method is tested on a radar system operating in the 76-77 GHz band. This radar used a chirp sequence modulation with 128 ramps per measurement. As interferer, we used an FMCW radar with a triangular modulation scheme with a ramp duration of 1 ms. Its transmit frequency is kept constant from 76.4 to 76.45 GHz. The victim had a center frequency of 76.3 GHz with a bandwidth of 400 MHz.

Rising frequency ramps were transmitted, so interference occurs in the end of the baseband signal, shown in Fig. 7. The baseband signals of all 128 ramps are plotted into the figure to show the occurrence of interference over the complete measurement. A window function is applied, so the signal is curved. The threshold which was used to detect interference is drawn above and below the signal, the black box indicates detections. To the left of the detected interference, there are further artifacts in the signal. These are undesired side lines created by the interferer. They are lower in amplitude as the main signal and are below the detection threshold.

According to (1), $\hat{r}$ is calculated. It is higher than 0.5, so the radar shifts its center frequency to 76.2 GHz below the highest detected interfered frequency. In the time domain signal of the second measurement in Fig. 8 can be seen, that the high amplitude interference is not present anymore. Only the artifacts mentioned before are still visible, but damped by the window function.

V. Conclusion

A jamming avoidance response of bats to counteract interference was adapted to automotive chirp sequence radar. It was shown that the method outperforms a randomized frequency hopping and can be nearly as effective as a regulation of the frequency band. It works best if a high amount of frequency ramps is transmitted and if the ramp repetition intervals of interfering sensors are different. Additionally, the method can be easily combined with other interference countermeasures.

References

[1] N. Ulanovsky, M. B. Fenton, A. Tsoar, and C. Korine, "Dynamics of jamming avoidance in echolocating bats," *Proceedings of the Royal Society of London B: Biological Sciences*, vol. 271, no. 1547, pp. 1467–1475, 2004.

[2] M. Goppelt, H.-L. Blöcher, and W. Menzel, "Automotive radar - investigation of mutual interference mechanisms," *Advances in Radio Science*, vol. 8, pp. 55–60, 2010. [Online]. Available: http://www.adv-radio-sci.net/8/55/2010/

[3] T. Schipper, M. Harter, L. Zwirello, T. Mahler, and T. Zwick, "Systematic approach to investigate and counteract interference-effects in automotive radars," in *2012 9th European Radar Conference (EuRAD)*, Oct 2012, pp. 190–193.

[4] T. Schipper, M. Harter, T. Mahler, O. Kern, and T. Zwick, "Discussion of the operating range of frequency modulated radars in the presence of interference," *International Journal of Microwave and Wireless Technologies*, vol. 6, pp. 371–378, 6 2014.

[5] L. Mu, X. Zhang, T. Xiangqian, and Q. Liu, "A novel pn-coded fmcw radar design and implementation," in *2011 IEEE CIE International Conference on Radar (Radar)*, vol. 2, Oct 2011, pp. 1004–1007.

[6] M. Kunert, F. Bodereau, M. Goppelt, C. Fischer, A. John, T. Wixforth, A. Ossowska, T. Schipper, and R. Pietsch. (2010, June) Study on the state-of-the-art interference mitigation techniques. The MOSARIM Consortium. Page 8-9. [Online]. Available: https://assrv1.haw-aw.de/mosarim/index.php/component/remository/func-startdown/584/